Supplementary material to Comprehensive characterization of sooting butane jet flames, Part 2: temperature and soot particle size

I.A. Mulla[a,b], J. Yon[b], D. Honoré[b], C. Lacour[b], A. Cessou[b], B. Lecordier[b,*]

[a] *Department of Aerospace Engineering, Indian Institute of Science, Bangalore, 560012, India.*
[b] *Normandie Univ., UNIROUEN, INSA Rouen, CNRS, CORIA, 76000 Rouen, France*

S1. Thermocouple assessment

S1.1. Catalytic effect

Nearly identical inward and outward profiles imply no significant catalytic effects.

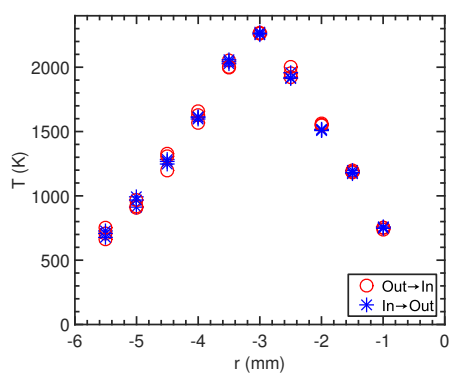

Figure S1: Temperature profiles with radially inward (oxidizer to fuel) and outward (fuel to oxidizer) traversing in Re 5000 flame at $y = 10\ mm$. The measurement duration is 3 s at each location.

*Corresponding author:
Email address: bertrand.lecordier@coria.fr (B. Lecordier)

S1.2. Soot deposition effect

Nearly constant trace suggests negligible soot deposition, which was also confirmed through visual inspection.

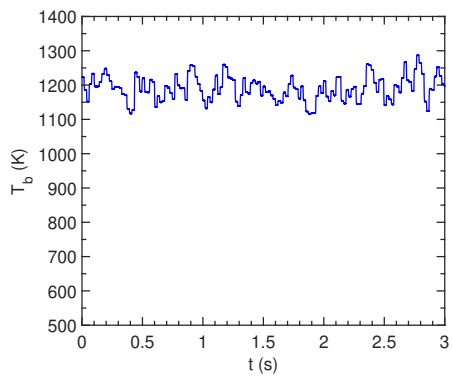

Figure S2: Thermocouple junction temperature history in Re 5000 flame at $r = -6\ mm, y = 120\ mm$. Mean f_v at this location measures 90 ppb.

S1.3. Radiation correction and velocity sensitivity

Thermocouple data is corrected for radiation heat loss by considering convection-radiation balance as, $T_g = T_b + (\sigma\epsilon_b T_b^4)/h$, where: T_g is gas temperature, T_b is thermocouple junction temperature, σ is Stefan-Boltzmann constant, ϵ_b is thermocouple emissivity, and h is convective heat transfer coefficient. ϵ_b is a function of temperature as, $\epsilon_b = 1.507\times10^{-4}(T_b) - 1.596\times10^{-8}(T_b^2)$ [1]. h is obtained using Kramer's expression for Nusselt number, $Nu = hD/k = 0.42Pr^{0.2} + 0.57Pr^{0.33}Re^{0.5}$, where: $Re = \rho V D_{th}/\mu$, $Pr = \mu C_p/k$, D_{th} is thermocouple wire diameter, k is thermal conductivity of gas, ρ is gas density, V is gas velocity, and μ is dynamic viscosity of gas. The gas properties are temperature dependent. Thus, T_g is computed iteratively. The properties of air are considered. The gas velocity V at a given radial (r) and downstream (y) locations is calculated using a turbulent jet modeling [2]. This model requires centerline velocity (V_{max}) which was obtained as, $V_{max} = C.V_{avg}$, where V_{avg} is the area-averaged velocity (V_{avg}) deduced from the imposed mass flow rate. The factor C depends on Re. For Re 21500 case, C was found to be 1.16 through

the velocity measurement (data available in the Supplement of Part 1 [3]). For Re 5000 and 7200 cases, C values are assumed to be 2 and 1.5, respectively. As the velocity model [2] is valid only for non-reacting jets, a factor of four is used for Re 5000 and 7200 cases to account for the gas expansion induced velocity jump in reacting flows based on [4]. For the Re 21500 case, since the temperature was lower at measurement locations, the velocity jump factor is assumed to be 3.

To justify various assumptions, we performed a sensitivity analysis for a range of velocities and thermocouple junction temperatures. The sensitivity map is shown in Fig. S3. The effect of velocity error is primarily relevant at high temperature ($> 1800\ K$) and low velocities. Therefore, the uncertainty impact is relevant at peak flame temperatures ($> 2000\ K$). The present work mainly focuses on the soot and PAH formation temperature range ($600 - 1600\ K$), which is lower than the flame temperature. Therefore, uncertainty is expected to be low. Other sources of uncertainty are discussed subsequently.

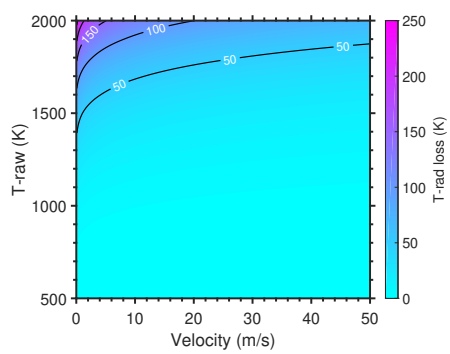

Figure S3: Radiation correction sensitivity as a function of probe temperature and gas velocity. Isolines are overlaid at every 50 K.

S1.4. Temperature uncertainty estimate

The uncertainty in temperature measurement can arise primarily from the following sources.

1. Radiation correction: Uncertainty in radiation correction due to various ap-

proximations is discussed. The velocity in the present flames was sufficiently high. Therefore, the errors in radiation correction were negligible (0.5%, when velocity is changed by half) even at a high temperature (2250 K). Another source of error is due to the size of the thermocouple junction diameter [5]. The butt-welded junction diameter for one of the thermocouples was observed (with a digital microscope) to be lower (35 μm) than the wire diameter (50 μm). This can lead to errors up to 5% at peak temperature (2250 K), while the error is negligible at low/moderate temperatures ($0.1 - 1.5\%$ for $600 - 1600$ K). In the $600 - 1600$ K temperature range, error in radiation correction from other sources (emissivity, Nu number correlations, considering only air properties) is expected to be negligible due to the small thermocouple size.

2. Positional error: Thermocouple was positioned with respect to the flame axis through 2D mapping, as described in the accompanying paper. A motorized translation with a resolution (1 μm) better than the thermocouple junction diameter was used. Therefore, the positioning accuracy is estimated to be the same as the thermocouple wire diameter (50 μm). This positional error in the steep gradient region (at 1400 K) translates to 40 K uncertainty. Therefore, 3% uncertainty is assigned to the positional error.

3. Statistical uncertainty: Uncertainty in mean owing to flame fluctuations was estimated by considering the standard deviation ($S.D.$) and the number of samples (N) as $2S.D./\sqrt{N}$ (95% confidence interval). Thermocouple data was acquired over 3 s duration at 3 kHz rate; however, the response time of the thermocouple is estimated to be 10 ms. Therefore, the effective number of time decorrelated samples is reduced to 300. Consequently, uncertainty in the mean is estimated to be ± 0.05 to 3%, depending on a location within the flame. We chose a conservative value of $\pm 2.5\%$ for all the measurements.

Following the uncertainty propagation principle, the total uncertainty of $\pm 6\%$ is estimated in mean temperature at a peak value (2250 K), while $\pm 4\%$ in the temperature range of $600 - 1600$ K.

S2. SMPS probe

S2.1. Flame with sampling probe

Figure S4 shows flame photographs with the probe, suggesting low global perturbations.

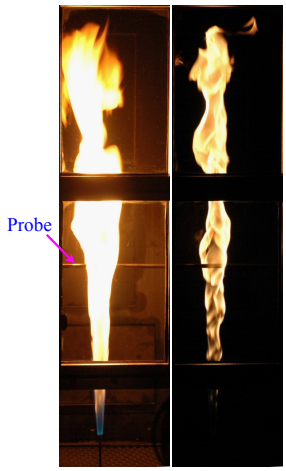

Figure S4: *Re* 7200 flame photographs with SMPS/PPS sampling probe at $y = 250\ mm$. Images with two exposures, namely 1/20 s (left) and 1/500 s (right) are shown.

S2.2. Orifice blockage correction

The temporal evolution of soot volume fraction in the extracted aerosol sample from *Re* 7200 flame is provided in Fig. 10 of the paper. It is evident that the SMPS measurements are affected by the probe blockage over time. Therefore, the SMPS data is corrected using the f_v trace from PPS measurements. SMPS scans different classes (bins) of mobility diameters sequentially, and respective number concentrations are measured simultaneously by a Condensation Particle Counter (CPC). Thus, the number concentrations measured by CPC during the scan time are linked to respective mobility diameter bins. By assuming that the orifice blockage only affects the aerosol number concentration (and not the particle size), the CPC number counts can be corrected by using the f_v trace as a function of time. The SMPS data until 60 nm with a corresponding time duration of 75 s is considered. The PPS f_v trace over the same duration (75 s) as

of SMPS scan is extracted. To remove the high-frequency noise, Savitzky–Golay filter is applied to the PPS trace before using it for the SMPS correction. Next, the CPC counts are divided by the peak normalized f_v at respective scan times. In this manner, the correction strategy reconstructs the particle size distribution (PSD) by accounting for the orifice blockage over time.

Figure S5 shows the PSD with and without the blockage correction. Recall, SMPS measurements are intended only for the particle sizing and not the concentration (which is provided by PPS or laser-induced incandescence data from Part 1 [3]). Therefore, the particle concentration in Fig. S5 is not corrected for dilution. SMPS data is primarily used to obtain the mode (most probable) diameter. Both the corrected and uncorrected PSD conforms to the log-normal distribution in Fig. S5. However, the mode diameter in corrected data appears to be slightly higher, although the difference is not significant. This is due to the relatively short scan duration (75 s until 60 nm) compared to the orifice blockage timescale shown in Fig. 10. Similar to Fig. S5, data for all other cases are corrected for orifice blockage. The PSD of uncorrected and corrected data at different heights for Re 5000, 7200, and 21500 flames are provided in Sec. 3.4.1 of the paper.

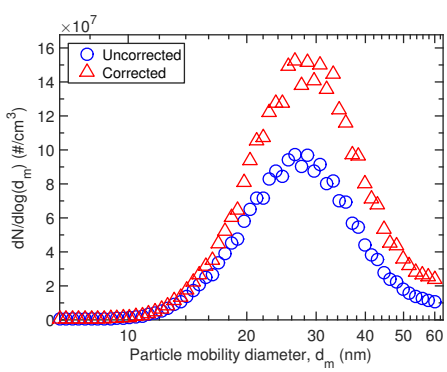

Figure S5: Probe blockage correction applied to SMPS data for $Re = 7200$ flame at $r = 0\ mm$, $y = 250\ mm$.

References

[1] V. J. Lyons, C. M. Gracia-Salcedo, Determination of combustion gas temperatures by infrared radiometry in sooting and nonsooting flames, Tech. Rep. NASA-E-4446, National Aeronautics and Space Administration Cleveland OH Lewis Research Center (1989).

[2] G. Xu, R. Antonia, Effect of different initial conditions on a turbulent round free jet, Exp. Fluids 33 (5) (2002) 677–683. doi:10.1007/s00348-002-0523-7.

[3] I. Mulla, B. Lecordier, P. Desgroux, A. Cessou, Comprehensive characterization of sooting butane jet flames, Part 1: soot, soot-precursor, and reaction zone, Combust. Flame , in press (2021) xxx–xxx.

[4] G. R. Ruetsch, L. Vervisch, A. Liñán, Effects of heat release on triple flames, Phys. Fluids 7 (6) (1995) 1447–1454. doi:10.1063/1.868531.

[5] B. Ma, G. Wang, G. Magnotti, R. S. Barlow, M. B. Long, Intensity-ratio and color-ratio thin-filament pyrometry: Uncertainties and accuracy, Combust. Flame 161 (4) (2014) 908–916. doi:10.1016/j.combustflame.2013.10.014.